

Y. B. Liu
O. Batelaan
F. De Smedt
N. T. Huong
V. T. Tam

Test of a distributed modelling approach to predict flood flows in the karst Suoimuoi catchment in Vietnam

Received: 7 June 2005
Accepted: 15 June 2005
Published online: 20 September 2005
© Springer-Verlag 2005

Y. B. Liu (✉) · O. Batelaan
F. De Smedt
Department of Hydrology
and Hydraulic Engineering,
Vrije Universiteit Brussel, Pleinlaan 2,
1050 Brussels, Belgium
E-mail: yongbliu@vub.ac.be
Tel.: + 32-2-6293335
Fax: + 32-2-6293022

N. T. Huong · V. T. Tam
Research Institute of Geology
and Mineral Resources,
Thanh Xuan, Hanoi, Vietnam

Abstract The major obstacles for modelling flood processes in karst areas are a lack of understanding and model representations of the distinctive features and processes associated with runoff generation and often a paucity of field data. In this study, a distributed flood-modelling approach, WetSpa, is modified and applied to simulate the hydrological features and processes in the karst Suoimuoi catchment in north-west Vietnam. With input of topography, land use and soil types in a GIS format, the model is calibrated based on 15 months of hourly meteorological and hydrological

data, and is used to simulate both fast surface and conduit flows, and groundwater discharges from karst and non-karst aquifers. Considerable variability in the simulation accuracy is found among storm events and within the catchment. The simulation results show that the model is able to represent reasonably well the stormflows generated by rainfall events in the study catchment.

Keywords Flood prediction · WetSpa · GIS · Karst Suoimuoi catchment · Vietnam

Introduction

Modelling of karst hydrology in a catchment has been less successful for hydrologists due to strong physical and geometrical heterogeneities of the karst aquifer, which cause complex hydraulic conditions and spatial and temporal variability of the model parameters. Generally, two processes, quick flow and slow flow, are apparent and control the characteristics of a karst stormflow hydrograph. After a storm, rapid and turbulent groundwater recharge and drainage occur primarily in large conduits through which a large amount of infiltrated water moves rapidly to a karst spring, while slow and predominantly laminar drainage occurs due to gradual emptying of pores, smaller fractures and fissures (Jukic and Jukic 2003). As pointed out by Labat et al. (2000), a karst aquifer can be thought as composed of three interacting systems: the soil forming the upper non-karst impluvium, followed by the infiltration zone

to a few metres below the ground surface, which is composed of fine fractures where both unsaturated and saturated flow may occur, and finally, the low permanently saturated karst zone composed of a highly organized and hierarchized drainage conduit system in connection with a network of secondary drains. The outlet of the conduit system is a spring. The open conduit provides low resistance pathways for the subsurface flow, which often has more in common with surface water than with groundwater. Therefore, karst hydrology requires concepts of both surface water and groundwater hydrology (White 2002).

In recent decades, progress has been made in the use of water budgets, tracer studies, hydrograph analysis and chemograph analysis for the characterization of karst aquifers. These have improved the understanding of karst properties, characteristics and evolution substantially. In general, three types of hydrological models can be divided in simulation of karst hydrology:

physical models, conceptual models and empirical models (Jukic and Jukic 2003). Physical models (e.g. Adams and Parkin 2002, Eisenlohr et al. 1997) are based on principles and formulas valid for turbulent laminar flows in porous media. To provide numerous input data and model parameters, the distribution and geometry of fractures in a karst aquifer need to be investigated, which is very difficult to access by direct observation. This has resulted in a wide use of conceptual models in karst hydrology, for instance Juberias et al. (1997), Haliban and Wicks (1998) and Cheng and Chen (2005). Conceptual models are based on the conceptualization of the karst aquifer as a configuration of internal storages and pathways, while physical relationships are not considered explicitly but are represented in general terms through the conceptualization of the aquifer. Empirical or black-box models use mathematical relations between input and output time series without applying physical laws, for which the linear transfer function between rainfall and runoff is commonly applied to represent the unit response function of the karst aquifer. However, many models are not clearly defined as belonging to anyone of these categories, but possess a combination of components from different classes. The choice of simulation model thus depends on project objectives, data availability, geophysical characteristics of the karst catchment, etc.

Differing from non-karst catchment, storm runoff is to a large extent provided by water flowing the subsurface routes to the streams in a karst catchment, either through the soil matrix or within the fractured bedrock, while surface runoff is very small to negligible (Majone et al. 2004). Moreover, diverse pathways exist in the shallow subsurface and in the underlying rock formation resulting in a broad distribution of travel times from the land surface to the outlet springs. As a result, inference of travel time statistics from spring hydrographs is fraught with difficulties. The most critical are the non-linear effects due to soil moisture dynamics and prevent water contribution during stormflow (Labet et al. 2000). Modelling such a complexity is a quite challenging task, which is typically tackled by means of simplified rainfall-runoff models (Majone et al. 2004). This implies that runoff generation is inherently linear and time-invariant, and the total hydrograph can be decomposed into simple elements and can be estimated by the linear convolution integral between effective rainfall and a physical transfer function. However, successful application of this simplified scheme depends on many other factors, such as the quality of input and output time series, data availability of catchment geomorphology, lithology, channel geometrics, etc.

This paper presents an adapted modelling approach for simulation of stormflow in the karst Suoimuoi catchment, Vietnam, using a GIS-based spatially distributed hydrological model, WetSpa (Liu et al. 2003,

Liu 2004). The modifications made to WetSpa to simulate karst aquifers are (1) the addition of a preferential “bypass” flow mechanism to represent vertical infiltration through a high-conductivity soil layer, (2) the coupling of surface water routing features to the conduit system, (3) the coupling of a non-linear reservoir model to a variably saturated groundwater component. The modelling processes and parameters are adjusted separately for the limestone and non-limestone areas based on 15 months of hourly meteor–hydrological data. Encouraging results have been achieved by comparison of measured and simulated hydrographs at the catchment outlet.

The study catchment and data availability

The Suoimuoi catchment is situated in the mountainous Da River basin in the northwest Vietnam. It covers an area of 273 km² with the Suoimuoi sinkhole as the catchment outlet. The catchment is confined in two regional deep fault systems trending in NW–SE direction, the Son La Fault on the east and the Da River Fault on the west. About 60% of the catchment is covered by karst features with different limestone formations as shown in Fig. 1. There is almost no surface water drainage in the karst area. Instead, closed depressions exist with cave systems developed in the bottom or in the rock walls (Tam et al. 2004). The karst aquifers receive water, mainly by the regional groundwater flow, with additional important in-situ recharge by rainfall, surface water and exotic water from higher-lying non-karst areas. The movement of karst groundwater is closely controlled by these tectonic deformations. The ground-

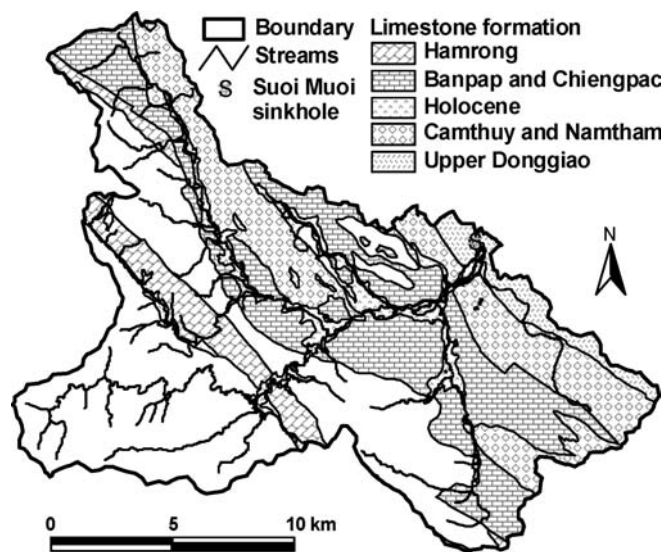


Fig. 1 Distribution of karst limestone in the Suoimuoi catchment

water is mainly stored in fractures, crushed zones and caves, and circulates in consistence with the hydrodynamic variation. There exist a number of karst springs/resurgences and sinkholes along the river course, which play a role in interaction between karst groundwater and surface runoff (Tam et al. 2001).

The Suoimuoi catchment is characterized by a humid subtropical climate, and is heavily influenced by the monsoon regime in the northern Vietnam. Two distinct seasons can be observed in the area: the dry winter lasting from November to April, and the rainy summer from May to October. The yearly mean temperature is 21.1°C with an observed maximum temperature of 41°C and minimum temperature of 1.1°C. In the study region, the mean annual precipitation is 1,450 mm, about 85% of which falls during the rainy season in summer.

During the period 2000–2003, an extensive hydrological and geophysical survey was conducted to study the mechanisms of hydrogeological processes in the Suoimuoi catchment. Many sophisticated methods, such as computer modelling, hydrogeological mapping, tracer and pumping test, etc., were performed to analyse complex groundwater systems. However, it was found that more data are needed to make the methods work perfectly in this highly heterogeneous system (Tam et al. 2004). The drainage area of the catchment is delineated by integration of remotely sensed imagery with ground surveys conducted by Hung et al. (2002). Three digital maps, DEM, soil type and land use, available in raster format are used to derive spatial model-parameters required in the WetSpa model. The elevation data for the river basin was digitized from an elevation map and interpolated to construct a 50×50 m grid size DEM (Fig. 2). The topography of the catchment is characterized by highlands in the upper part and lowlands in the lower part of the catchment. Elevation ranges from 539 to 1815 m with an average catchment slope of 33.2%. The land use consists of close canopy forest (1.7%), open canopy forest (4.2%), shrub (40.4%), grass land (5.6%), upland fields (38.3%), paddy fields (5.2%), residential area (4.5%) and open water (0.01%) (Fig. 3). Major soil types in the catchment are clay (64.3%), clay loam (22.3%), silt loam (11.7%) and sand (1.7%).

A 15-month-observed hydro-meteorological data from January 2000 to March 2001 are used to calibrate model parameters in this study. The hourly stream flow into the Suoimuoi sinkhole was captured by an automated water-level logger. The recorded hourly series of water level was converted to flow hydrograph by a well-calibrated rating curve. The resulting hydrographs are used in the baseflow separation and the model validation. Hourly precipitation was monitored by an automated logger located 4 km upstream of the Suoimuoi sinkhole, and was assumed to be uniformly distributed over the catchment. In addition, the data of potential evapotranspiration and air-temperature were collected

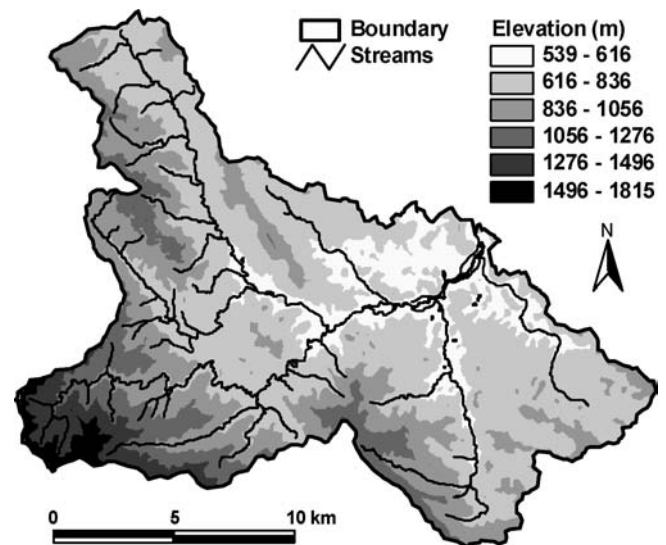


Fig. 2 Topographic map of the Suoimuoi catchment

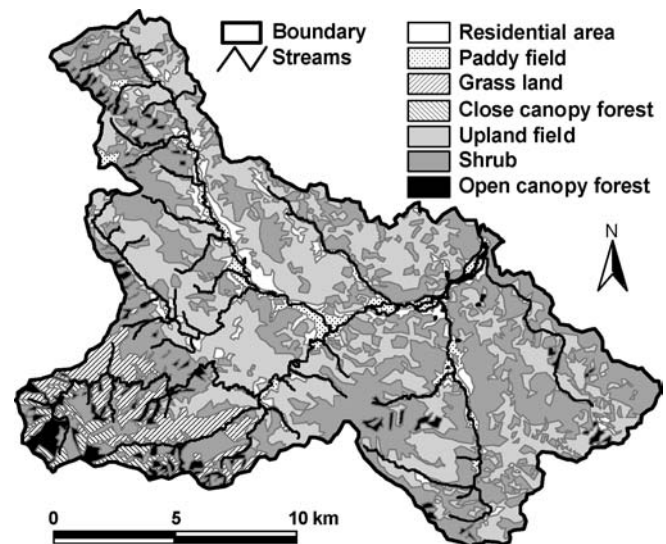


Fig. 3 Land use map of the Suoimuoi catchment

from a nearby gauging station, which are used as input to the model.

Methodology and application

Description of the WetSpa model

WetSpa is a grid-based distributed hydrologic model for water and energy transfer between soil, plants and atmosphere (Liu et al. 2003). For each grid cell, four layers are divided in the vertical direction as vegetation zone, root zone, transmission zone and saturated zone.

The hydrologic processes considered in the model are precipitation, interception, depression, surface runoff, infiltration, evapotranspiration, percolation, interflow, groundwater flow and water balance in the root zone and the saturated zone. The total water balance for a raster cell is composed of the water balance for the vegetated, bare-soil, open water and impervious parts of each cell. The model predicts peak discharges and hydrographs, which can be defined for any numbers and locations in the channel network, and can simulate the spatial distribution of catchment hydrological variables.

Surface runoff is calculated in the model by a modified rational method as:

$$R_s = C_p P_n (\theta / \theta_s) \quad (1)$$

where R_s [LT^{-1}] is the rate of surface runoff, C_p [-] is a potential runoff coefficient, P_n [LT^{-1}] is the rainfall intensity after canopy interception, θ and θ_s [L^3L^{-3}] are actual and saturated soil moisture content, and α [-] is an empirical exponent. The potential runoff coefficient C_p is a measure of rainfall partitioning capacity, depending upon slope, soil type and land use combinations. Default potential runoff coefficients for different slope, soil type and land cover are interpolated from literature values, and a lookup table has been built relating potential runoff coefficient to different combinations of slope, soil type and land use (Liu 2004). The effect of rainfall duration is also included in the model, as more runoff is produced during a storm event due to increasing soil moisture content. In general, the equation accounts for the effect of slope, soil type, land use, soil moisture, rainfall intensity and its duration on the production of surface runoff in a realistic way.

The routing of overland flow and channel flow is conducted by an approximate solution to the diffusive wave equation in the form of a density function of the first passage time distribution (Liu et al. 2003), which relates the discharge at the end of a flow path to the available runoff at the start of the flow path:

$$U(t) = \frac{1}{\sqrt{2\pi\sigma^2 t^3 / t_0^3}} \exp \left[-\frac{(t - t_0)^2}{2\sigma^2 t / t_0} \right] \quad (2)$$

where $U(t)$ [T^{-1}] is the flow path unit response function, t_0 [T] is the flow time, and σ [T] is the standard deviation of the flow time. The parameters t_0 and σ are spatially distributed, and are obtained by integration along the topographically determined flow paths as a function of flow celerity and dispersion coefficient (Liu et al. 2003).

Water balance in the root zone is modelled by equating input and output. Water infiltrated into the soil may stay as soil moisture content, move laterally as interflow or percolate as groundwater recharge depending on the moisture content of the soil. Both percolation and interflow are assumed to be gravity-driven in the model.

Percolation out of the root zone is equated as the hydraulic conductivity corresponding to the moisture content as a function of the soil pore size distribution index, and is expressed as:

$$R_g = K_s \left(\frac{\theta - \theta_r}{\theta_s - \theta_r} \right)^{(2+3B)/B} \quad (3)$$

where R_g [LT^{-1}] is the percolation out of root zone, K_s [LT^{-1}] is the saturated soil hydraulic conductivity, θ_s [L^3L^{-3}] is the soil porosity, θ_r [L^3L^{-3}] is the residual moisture content, and B [-] is the soil pore size distribution index. Interflow is assumed to occur in the root zone after percolation and becomes significant only when the soil moisture is higher than field capacity. Darcy's law and a kinematic approximation are used to estimate the amount of interflow, in the functions of hydraulic conductivity, the moisture content, the slope angle and the root depth. The actual evapotranspiration from soil and plant is calculated as a function of potential evapotranspiration, vegetation and stage of growth and moisture content. A percentage of the remaining potential evapotranspiration is taken out from the water content in the groundwater reservoir as a function of the maximum reservoir storage, giving the effect of a steeper baseflow recession during dry period. Groundwater flow is modelled using a linear reservoir method on small subcatchment scale. The groundwater outflow is added to any runoff generated at the subcatchment outlet to produce the total streamflow. Hence, the flow routing consists of tracking runoff along its topographically determined flow path, and evaluating groundwater flow for each small subcatchment. The total discharge at the catchment outlet is obtained by summation of the overland flow, interflow and groundwater flow.

Model modification for karst areas

Apparently, the schemes of WetSpa model are not valid in simulating hydrological processes in a karst catchment. Stormwater in karst areas may flow overland from ridge tops, and then enter the ground in upland regions through recharge features and resurgent at springs in low areas. Diffuse infiltration can also take place through the soil and the underlying epikarst. On steep slopes that do not readily develop sinkholes, diffuse infiltration can occur through the soil or into bedrock fissures. In addition, it is difficult to identify groundwater flow paths and divisions in karst aquifers which arise from the extreme heterogeneity and anisotropy of the karst aquifer, and from changes in groundwater patterns with different stages of flow. Taking the above specific characteristics into account, some major modifications are made to the WetSpa model in order to

better represent the predominant hydrological features in karst areas in the Suoimuoi catchment.

To reflect the fact that almost no surface flow is apparent in karst areas, the surface runoff coefficient in karst areas is set to zero in the model, which implies that all stormwater after canopy interception infiltrates into the soil. The water in the root zone remains temporarily stored in the soil, and is depleted by evapotranspiration, conduit flow through the underlying epikarst, and recharge to the groundwater reservoir. Due to the coarse soil texture and the well-developed fracture systems in the bedrock, vertical flow is considered to be predominant in the soil layer, and the interflow scale factor is set to zero in the modified WetSpa model assuming that no interflow occurs in the root zone layer.

Evidence has shown that karst drainage and conduit development are usually aligned along favourable lithostratigraphic horizons and zones of fracture. However, the amount of water that contributes to conduit runoff through fine fractures and pores is strongly affected by the overlying soil and landscape characteristics (Urich 2002). The primary impact is the resulting change of water volume out of the root zone, which eventually affects the fracture development in the epikarst and karst layers forming pathways to transfer water into the rapid conduit and cave flow. Steep slopes usually mark topography next to rivers and are prone to mechanical failure and fracture development through time (Mullins and Hine 1989). In the Suoimuoi catchment, karst areas are mostly covered by clay soils, with mixed shrub vegetation in steep slopes and upland field in gentle slopes. This implies that the runoff contributing to fast conduit flow follows the same trend as surface runoff generated in non-karst areas. A similar concept has been proposed by Kaufmann and Braun (2000) for the study of karst aquifer evolution by assuming the recharge rate proportional to the surface runoff. To keep the consistency of WetSpa model, the runoff that contributes to fast conduit flow is estimated as a linear function of the potential runoff coefficient corresponding to the same slope, soil type and land use characteristics but for non-karst areas, and is proportional to the amount of groundwater recharge, i.e.:

$$R_c = K_c C_p R_g \quad (4)$$

where R_c [LT^{-1}] is the amount of water that contributes to conduit flow, and K_c is a lumped correction factor that can be optimized during model calibration, or estimated from the observed hydrographs by proper flow-separation techniques. In such a way, the fast conduit runoff is directly linked with the characteristics of site slope, soil type, land use and soil moisture content, and therefore can be simulated using a spatially distributed model.

Conduit flow is strongly influenced by structurally controlled fractures, which connect surface and sub-surface, and provide for rapid flow through the aquifer to the discharge points. It is similar to the flow in a surface stream in that both are convergent through a system of tributaries and both receive diffuse flow through the adjacent soils or bedrock (Labat et al. 2000). Routing of conduit flow in a karst system is difficult due to its non-Darcian flow behaviour and complex flow paths. To simplify, the concentration time of conduit flow from a site to the stream and the basin outlet is assumed to be proportional to the concentration time along its surface flow paths, while neglecting the complex properties of flow path, slope, hydraulic radius, etc., i.e.:

$$t_c = K_t t_0 \quad (5)$$

where t_c is the average travel time of conduit flow [T], and K_t [-] is a lumped correction factor for conduit flow travel time, which can be determined through the analysis of observed flow hydrographs or through model calibration. The standard deviation of the conduit flow time is then assumed to be in the same order of magnitude as the travel time. In such a way, the conduit runoff can be routed to the basin outlet while keeping the consistency of flow routing schemes used in the WetSpa model.

To account for the complexities of both karst and epikarst groundwater system, which determines the slow flow response at the basin outlet, a non-linear reservoir model is applied for the karst areas on small subcatchment scale, i.e.:

$$Q_g = K_1 G + K_2 G^2 \quad (6)$$

where Q_g [$L^3 T^{-1}$] is the groundwater discharge at the subcatchment outlet, G [L^3] is the average active groundwater storage of the subcatchment, K_1 [T^{-1}] and K_2 [$L^{-3} T^{-1}$] are the first- and second-order baseflow recession constant. These two parameters can be obtained through the analysis of observed flow hydrographs, and can also be optimized through model calibration.

Through the above major modifications to the WetSpa model, the spatial distribution of runoff and flow responses can be simulated in karst areas. Though the conceptual basis of such modifications cannot fulfil the requirement of identifying karst hydrological features in detail, the model provides a reasonable tool for predicting flood flows by coupling catchment topography, soil type and land use characteristics in a karst catchment. The total hydrograph at the catchment outlet is then obtained by summation of the direct flow, interflow and groundwater flow from the non-karst areas and the conduit flow and groundwater flow from the karst areas.

Parameter identification and optimization

Model parameters are identified firstly, using GIS tools and lookup tables which relate default model parameters to the base maps or the combination of base maps. Starting from the 50 by 50 m pixel resolution digital elevation map, hydrological features including surface slope, flow direction, flow accumulation, flow length, stream network, drainage area and subcatchments are delineated. The threshold for determining the stream network is set to 50, i.e. the cell is considered to be drained by streams when the total drained area becomes greater than 0.125 km². The threshold for delineating subcatchments and main streams is set to 1,000. Maps of porosity, field capacity, wilting point, residual moisture, saturated hydraulic conductivity and pore size distribution index are obtained from the soil type map. Maps of root depth, Manning's roughness coefficient and interception storage capacity are derived from the land use map. Maps of default runoff coefficient and depression storage capacity are calculated from the slope, soil type and land use class combinations.

The residential areas are mainly distributed besides the Suoimuoi river channel as villages or small towns. Due to the grid size, the residential cell is assumed to be 10% covered by impervious materials (roof, road, etc.), and the rest covered by farmland. The average flow depth is estimated using the power law relationship with an exceeding probability of a 2-year return period resulting in a minimum overland flow depth of 0.005 m and the channel flow depth of 1.0 m at the catchment outlet (Liu et al. 2003). By combining the maps of the average flow depth, Manning's roughness coefficient and surface slope, the average flow velocity in each cell is calculated using Manning's equation, which results in a minimum value of 0.005 m/s for overland flow, and up to 2.5 m/s for some parts of the main river. Next, the celerity and dispersion coefficient at each cell are produced, and the values of concentration time and its standard deviation for each contributing cell are generated. With the above information, the unit flow path response functions are calculated from each cell to the sub-basin outlet and from the sub-basin outlet to the basin outlet.

In dealing with the specific problems of karst areas in the Suoimuoi catchment, the map of potential surface runoff coefficient is set to zero on those areas. Other parameters such as interflow scaling factor, conduit flow factor, concentration time factor, evapotranspiration factor, baseflow recession constants, etc., as listed in Table 1, are set or calibrated during model calibration.

Model calibration is implemented by comparing the simulated and observed hydrographs. Each of the correction factors and functions that involved the use of coefficients are determined using an independent automated model optimization process (Doherty and

Table 1 Lumped model parameters required for optimization

Parameter	Description	Value
K_c	Correction factor for conduit runoff [-]	0.35
K_t	Correction factor for conduit flow travel time [-]	1.8
K_e	Correction factor for plant potential evapotranspiration [-]	1.13
K_1	First order baseflow recession constant [d ⁻¹]	0.015
K_2	Second order baseflow recession constant [m ⁻³ d ⁻¹]	0.0003
H_0	Initial active groundwater storage on subcatchment scale [mm]	200
H_{max}	Maximum active groundwater storage on subcatchment scale [mm]	300
S_0	Initial relative soil moisture content [-]	0.5

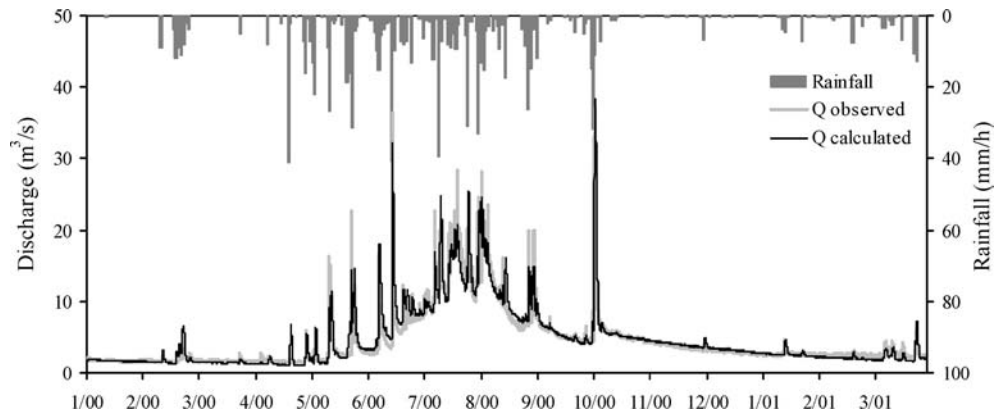
Johnston 2003). The objective function is the sum of squares of the difference between observed and predicted flows at the Suoimuoi sinkhole. The correction factor for estimating the volume of conduit flow is found to be around 0.35, and the concentration time of conduit flow is about 1.8 times of the surface runoff. This results in an average quick flow concentration time of 12 h and average standard deviation of 8 h for the entire catchment. Next, a manual calibration is applied to refine model parameters by a trial-and-error method. The trial-and-error procedure can be applied because the number of calibrated parameters is limited, and the majority of the proposed parameters have physical meaning and relatively short ranges. The two baseflow recession constants at the catchment outlet are initially estimated from the recession curves in the observed hydrograph, and refined during calibration. These values are then adjusted for each subcatchment based on its slope, drainage area and geological features (Liu 2004).

Results and discussion

Flow prediction at the Suoimuoi sinkhole

A graphical comparison between observed and predicted hydrographs for the simulation period at the Suoimuoi sinkhole is presented in Fig. 4. One can find a reasonable agreement between simulation results and the observed hydrograph. But for some of the floods, as for instance the floods in May and August 2000, the peaks are less accumulatively estimated. The highest rainfall intensity was 41 mm/h, observed on 26 April 2000, but this storm did not produce a high flood, because the antecedent soil moisture was very low leading to high water storage in the soil. The largest flood occurred on 6 October 2000, with a maximum rainfall intensity of 31 mm/h and an

Fig. 4 Observed and calculated hydrographs at Suoimuoi sinkhole



accumulated rainfall of 146 mm in 22 h. Due to the high antecedent soil moisture condition, this storm caused a severe flood with an observed peak discharge of 37.1 m³/s. The calculated peak discharge is 38.4 m³/s, which is 3.5% overestimated. Also, the delay time of peak occurrence is 3 h, which is well-estimated by the model.

For the 15-month simulation results, about 10% of the total rainfall is lost by interception, 54% of the total rainfall returns to the atmosphere as evapotranspiration from the soil and groundwater storage, and 36% becomes runoff, which is mainly generated during the wet season. The simulated flow volume is composed of surface runoff (7%) from non-karst areas, residential areas and open water surface, fast conduit runoff (10%) from karst areas, and groundwater flow (83%) from karst and non-karst areas. The runoff from non-karst areas contributes to about 19% of the total river discharge calculated at the Suoimuoi sinkhole. This is because non-karst areas exhibit more evapotranspiration than karst areas due to their higher soil-water-holding capacity, and part of its groundwater drains into downstream karst aquifers. However, its discharge contribution can increase to 32% of the total river discharge during storms, due to surface runoff and interflow generated from steep terrains. This result is similar to that obtained by Tam et al. (2001) based on river discharge measurement.

Four statistical evaluation criteria were applied to the 15-month simulation results to assess the model performance. It is found that the modified WetSpa model reproduces the observed water volume with -2.4% underestimation. The model Nash efficiency (Nash and Sutcliffe 1970) for reproducing the river discharges is 72%. The two adapted Nash efficiencies proposed by Hoffmann et al. (2004) for reproducing low and high flows are 72% and 76% respectively. Regardless of the acceptable evaluation results, the model contains many uncertainties, such as deficiencies in model structure, boundary conditions and errors associated with measurements used in model calibration. Weaknesses in the

model structure are the simplification in describing the surface runoff production, conduit flow, soil moisture relationships with actual evapotranspiration, flow routing procedures, etc. In particular, the model applies a linear convolution integral for fast flow routing in the karst and non-karst system. This implies that the system is considered as time-invariant, and the property of proportionality and superposition law are valid, i.e. the sum of separate hydrographs directly forms the total hydrograph and vice versa. These two hypotheses in the model may result in high irregularities in the obtained transfer functions and uncertainties in the modelling results. In addition, data errors associated with measurements and an insufficient number of meteorological stations in the catchment are also major sources of model uncertainty. Hence, errors in input data used for model calibration may result from treating rainfall and potential evapotranspiration as average values of those occurring throughout the catchment.

Fast runoff distribution and water balance

A simulated spatial distribution of fast runoff, i.e. the surface runoff from non-karst areas and conduit runoff from karst areas, for the storm-flood on 5–7 October 2000, is presented in Fig. 5. Due to the large volume and high intensity of the rainfall, storm runoff generated from almost all areas in the catchment. However, fast runoffs were mainly produced from steep slopes in non-karst areas as overland flow and in karst areas as fast conduit flow, and partly from residential areas and open water surface in the downstream river valley. The calculated average surface runoff in non-karst areas of the catchment is 14.8 mm (34% of the total fast runoff) forming the flood peak of the hydrograph. The calculated average conduit runoff in karst areas is 16.5 mm (59% of the total fast runoff) consisting the major recession part of the hydrograph, since its concentration time is longer than that of surface runoff from upstream

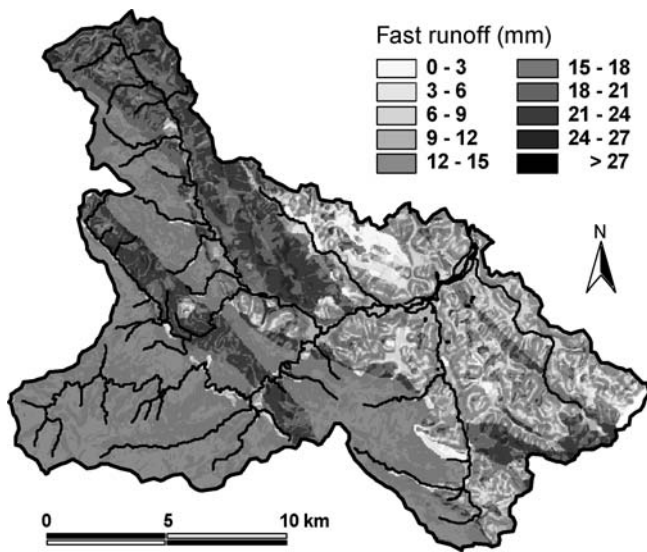


Fig. 5 Distribution of simulated fast runoff for the storm-flood on 5–7/10/2000

non-karst areas. The rest (7% of the total fast runoff) are from residential areas and open water surface in the catchment. The fast runoff generated in the eastern part of the catchment is rather small due to its sandy soil formation so that most of the infiltrated water contributes to groundwater storage and slow groundwater discharge in the following months. The spatial fast runoff distribution given by the model is in agreement with the Hortonian overland flow concept for the non-karst areas, and is related to the site's physical characteristics for karst areas. However, its validity is not verified due to lacking fast-flow observations at different sites.

For assessment of the catchment water balance and its seasonal variation of different fluxes, the hourly modelling outputs are integrated for each month as listed in Table 2. This includes the monthly precipitation

(P), the measured potential evapotranspiration (ET_0), the calculated actual evapotranspiration (ET_c), the observed discharge (Q_0), the calculated discharge from non-karst areas (Q_{nk}), the calculated discharge from karst areas (Q_k), the calculated total discharge (Q_c), the errors in discharge (ΔQ), the change of soil moisture content (ΔS) and the change of groundwater storage (ΔG). Other components, such as interception, infiltration, groundwater recharge, discharge, etc., are not presented in the table. A graphical presentation of the monthly precipitation, soil moisture and groundwater storage variation are given in Fig. 6.

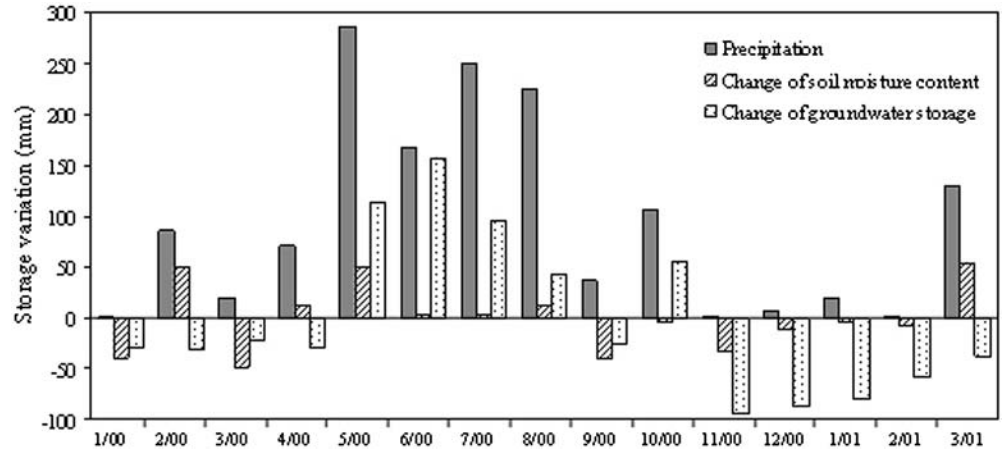
Figure 6 shows clearly that the rainy season in this area is from May to August, with a cumulative rainfall of 930 mm, which is 74% of the annual rainfall in 2000. This period is also the major groundwater recharge season, with a cumulative groundwater recharge of 406 mm or 88% of the annual recharge in 2000. The other recharge month is October in which a pronounced rainfall of 106 mm was recorded. Groundwater depletion lasts from November till April in a descending order. It is also evident from the figure that the soil or epikarst zone plays an important role in buffering and transferring rainwater into the groundwater system, as for instance in February 2000, and March 2001, where a pronounced rainfall was observed resulting in a significant increase of the soil moisture storage, which was afterwards used for evapotranspiration and groundwater recharge.

Based on the analysis of the baseflow at the Suoimuoi sinkhole by the method of Wittenberg (1999), it follows that the volume of baseflow is approximately 82% of the total streamflow volume within the simulation period. This high value shows that a major portion of the streamflow comes from groundwater, which is associated with shallow permeable soils and highly fractured bedrocks in the catchment. Analysis of the streamflow hydrograph shows that the fast runoff, which is considered to be composed of surface runoff from non-karst

Table 2 Monthly water balance for the Suoimuoi catchment (mm)

Month	P	ET_0	ET_c	Q_0	Q_{nk}	Q_k	Q_c	ΔQ	ΔS	ΔG
1/2000	1.20	71.5	56.6	12.2	0.75	9.65	10.4	1.80	-38.3	-28.7
2/2000	86.3	79.3	58.1	16.0	2.72	14.0	16.7	-0.70	49.6	-30.5
3/2000	21.1	101	76.4	18.1	1.83	15.1	16.9	1.20	-47.9	-21.6
4/2000	71.1	112	80.0	16.1	2.17	12.0	14.2	1.90	13.4	-27.9
5/2000	287	71.8	60.5	30.9	8.58	21.4	30.0	0.90	49.8	113
6/2000	168	60.4	58.9	53.7	13.7	44.6	58.3	-4.60	0.66	157
7/2000	249	64.3	65.1	132	32.1	95.0	127	5.00	0.58	94.2
8/2000	226	61.8	64.6	113	28.3	88.7	117	-4.00	12.3	42.1
9/2000	36.3	62.4	63.3	60.3	7.95	54.6	62.6	-2.30	-40.2	-26.1
10/2000	106	56.2	54.0	61.4	11.0	51.6	62.6	-1.20	-4.00	56.1
11/2000	1.80	69.1	68.7	37.2	3.10	36.6	39.7	-2.50	-33.6	-94.5
12/2000	7.50	68.3	66.6	29.6	3.49	30.1	33.6	-4.00	-10.3	-86.2
1/2001	18.3	81.0	76.2	25.9	3.09	23.3	26.4	-0.50	-3.22	-79.3
2/2001	1.80	74.4	60.0	21.9	1.48	16.6	18.1	3.80	-8.00	-58.0
3/2001	129	86.6	67.3	26.0	4.33	17.8	22.1	3.90	54.7	-36.9

Fig. 6 Monthly soil storage and groundwater storage deficit



areas and quick conduit flow in karst areas, terminates within 32 h after a major rainfall event, while the average peak time occurs around 10 h after the rainfall. This short flow time is due to the steep slopes and extensive conduit development in the downstream areas. Tam et al. (2004) conducted an analysis for the daily streamflow and rainfall series in the Suoimuoi catchment using auto-correlation and cross-correlation techniques and concluded that the time response or the mean residence time at the Suoimuoi sinkhole is 1 and 50 days for quick flow and baseflow respectively. The long baseflow residence time and its high proportion suggest that the karst groundwater system of the Suoimuoi catchment is governed by fractures and fissures. These results are compatible with present results obtained from the model simulation, which indicates that the modified WetSpa model is able to simulate both streamflow and water balance for the karst Suoimuoi catchment.

Summary and conclusion

A test of a GIS-based modelling approach for flood prediction in the karst Suoimuoi catchment is described in this paper. The model uses a modified rational method to calculate surface runoff in non-karst areas and conduit flow in karst areas based on the spatial characteristics of topography, soil type, land use and soil moisture condition. Flow into the outlet sinkhole is routed with a linear diffusive wave approximation method, while the concentration time of conduit flow is assumed to be proportional to the concentration time of the surface runoff. Total discharge at the basin outlet is

calculated by summing predicted fast runoff and groundwater flow from both non-karst and karst areas in the catchment. The model is calibrated using the 15-month hourly flow data series collected at the Suoimuoi sinkhole. The results of model calibration show that, in general, flow hydrographs well-predicted, especially the baseflow at the catchment outlet. However, predictions of peak discharge for some of the storms are less accurate indicating the need for improved methods of runoff volume calculation and flow routing in this catchment.

As discussed in the paper, the karst aquifers in the Suoimuoi catchment act as large underground reservoirs of water, but these reservoirs are difficult to exploit because little is known about their hydraulic behaviour. A simple hydrological model as the modified WetSpa model used in this study can provide useful information about the behaviour of such complex flow system. The model with alternative hypothetical structures allows to predict different runoff and flow components, which are fitted to observed hydrographs using an optimization algorithm. These results can be used to simulate the flow evolution, but do not allow to determine the internal structure and spatial disposition of contributions in the aquifer. From point of view of conceptual modelling, this explicitly acknowledges the lack of detailed information about the location and size of conduits and other flow paths. However, the model enables to predict the effects of topography, soil type and land use on runoff, recharge and groundwater discharge, and hence, to comprehend the hydrological behaviour of the river basin. Work continues on incorporating a more physical approach in estimation of runoff volume and flow transport to study the complex hydrological behaviour of the river catchment.

References

- Adams R, Parkin G (2002) Development of a coupled surface-groundwater-pipe network model for the sustainable management of karstic groundwater. *Environ Geol* 42:513–517
- Cheng JM, Chen CX (2005) An integrated linear/non-linear flow model for the conduit-fissure-pore media in the karst triple void aquifer system. *Environ Geol* 47:163–174
- Doherty J, Johnston JM (2003) Methodologies for calibration and predictive analysis of a watershed model. *J Am Water Resour Assoc* 39(2):251–265
- Eisenlohr L, Bouzelboudjen M, Kiraly L, Rossier Y (1997) Numerical versus statistical modeling of natural response of a karst hydrogeological system. *J Hydrol* 202:244–262
- Haliban T, Wicks CM (1998) Modeling of storm responses in conduit flow aquifers with reservoirs. *J Hydrol* 208:82–91
- Hoffmann L, El Idrissi A, Pfister L, Hingray B, Guex F, Musy A, Humbert J, Drogue G, Leviandier T (2004) Development of regionalized hydrological models in an area with short hydrological observation series. *River Res Appl* 20(3):243–254
- Hung LQ, Dinh NQ, Batelaan O, Tam VT, Lagrou D (2002) Remote sensing and GIS-based analysis of cave development in the Suoimuoi Catchment. *J Cave Karst Stud* 64(1):23–33
- Juberias TM, Olazar M, Arandes JM, Zafra P, Antiguada I, Basauri F (1997) Application of a solute transport model under variable velocity conditions in a conduit flow aquifer: Olalde karst system, Basque Country, Spain. *Environ Geol* 30:143–151
- Jukic VD, Jukic D (2003) Composite transfer functions for karst aquifers. *J Hydrol* 274:80–94
- Kaufmann G, Braun J (2000) Karst aquifer evolution in fractured, porous rocks. *Water Resour Res* 36(6):1381–1392
- Labat D, Mangin A, Ababou R (2000) Rainfall-runoff relations for karstic springs: Part I: Convergence and spectral analysis. *J Hydrol* 238:123–148
- Liu YB (2004) Development and application of a GIS-based distributed hydrological model for flood prediction and watershed management. Doctoral Thesis, Vrije Universiteit Brussel, Belgium
- Liu YB, Gebremeskel S, De Smedt F, Hoffmann L, Pfister L (2003) A diffusive transport approach for flow routing in GIS-based flood modelling. *J Hydrol* 283:91–106
- Majone B, Bellin A, Borsato A (2004) Runoff generation in karst catchment: multifractal analysis. *J Hydrol* 294:176–195
- Mullins HT, Hine AC (1989) Scalloped bank margins: beginning of the end for carbonate platforms. *Geology* 17:30–33
- Nash JE, Sutcliffe JV (1970) River flow forecasting through conceptual models, Part 1: A discussion of principles. *J Hydrol* 10:282–290
- Tam VT, Vu TMN, Batelaan O (2001) Hydrological characteristics of a karst mountainous catchment in the Northwest of Vietnam. *Acta Geologica Sinica* 75(3):260–268
- Tam VT, De Smedt F, Batelaan O, Darsargues A (2004) Study on the relationship between lineaments and borehole specific capacity in a fractured and karstified limestone area in Vietnam. *Hydrogeol J* 12(6):662–673
- Urich PB (2002) Land use in karst terrain: review of impacts of primary activities on temperate karst ecosystems. *Sci Conserv* 198:60p
- White WB (2002) Karst hydrology: recent developments and open questions. *Eng Geol* 65:85–105
- Wittenberg H (1999) Baseflow recession and recharge as nonlinear storage processes. *Hydrol Process* 13:715–726